Microascus cirrosus SZ 2021: A potentially new genotype of *Microascus cirrosus*, which can cause fatal pulmonary infection in patients with acute leukemia following haplo-HSCT

JIANJUN CHENG[1*], DAXIONG ZENG[1*], TING ZHANG[1*], LU ZHANG[1], XIU HAN[1], PENG ZHOU[1], LIN WANG[1], JUN HE[2,3] and QINGZHEN HAN[1]

[1]Center of Clinical Laboratory, Dushu Lake Hospital Affiliated to Soochow University, Soochow University, Suzhou, Jiangsu 215000; [2]Collaborative Innovation Center of Hematology, Soochow University, Suzhou, Jiangsu 215006; [3]Department of Human Leukocyte Antigen Laboratory, Jiangsu Institute of Hematology, First Affiliated Hospital of Soochow University, Suzhou, Jiangsu 215031, P.R. China

Received December 21, 2022; Accepted June 14, 2023

DOI: 10.3892/etm.2023.12103

Abstract. Uncommon *Microascus cirrosus (M. cirrosus)* species have been reported to cause an increasing number of subcutaneous and invasive fungal infections worldwide; since the first human infection was reported in 1992, seven cases have been reported in PubMed. The present study reports a novel genotype named *M. cirrosus SZ 2021* isolated from a patient undergoing hematopoietic stem cell transplantation, who exhibited extensive drug resistance and suffered a fatal pulmonary infection. This isolated *M. cirrosus* was cultured and determined by morphological observation, multi-locus sequence typing, matrix-assisted laser desorption and ionization time-of-flight mass spectrometry, and whole genome sequencing by next-generation sequencing. The whole nucleotide sequence (32.61 Mb) has been uploaded in the NCBI database (PRJNA835605). In addition, *M. cirrosus SZ 2021* was not sensitive to the commonly used antifungal drugs, including fluconazole, amphotericin B, 5-flucytosine and caspofungin. The current literature on human infections by *M. cirrosus* was reviewed to closely define the comprehensive clinical characteristics and etiological identification. In brief, the present study identified a new *M. cirrosus* and summarized the clinical characteristics of fungal pneumonia by *M. cirrosus* species. Complete laboratory identification methods from morphology to gene sequencing were also established for an improved etiological identification and further investigation into the real prevalence of invasive pneumonia by *M. cirrosus*.

Correspondence to: Dr Qingzhen Han, Center of Clinical Laboratory, Dushu Lake Hospital Affiliated to Soochow University, Soochow University, 9 Chongwen Road, Suzhou, Jiangsu 215000, P.R. China
E-mail: gyhqz2021@163.com

*Contributed equally

Key words: Microascus cirrosus, pulmonary infection, metagenomic next-generation sequencing, hematopoietic stem cell transplantation, multilocus sequence typing

Introduction

With the rapid development of medical technology, some hematological malignancies can be cured by hematopoietic stem cell transplantation (HSCT). To effectively avoid graft-versus-host disease (GVHD), the calcineurin inhibitors, ciclosporin or tacrolimus, are often used as long-term preventive drugs following transplantation (1). To destroy the normal immunity is inevitable, inhibiting the proliferation of T-cells, the maturation of dendritic cells and the activation of neutrophils (2,3). Therefore, the use of immunosuppressive agents following haploidentical HSCT (haplo-HSCT) leads to patients becoming susceptible to bacterial and fungal infections, which is the cause of increased non-relapse mortality in patients (4). Invasive fungal infection has caused serious fatal damage to patients who have undergone HSCT, including *Aspergillus* spp. and *Pneumocystis* (5,6). In addition to these common pathogens, patients are also vulnerable to some uncommon microorganisms following transplantation. Infections with rare pathogenic microorganisms are mainly described in case reports, and there is a lack of systematic research, including the analysis of conditions, diagnosis, treatment and traceability (7-10). As a result, the accurate identification of pathogens and the optimal management of uncommon disseminated fungal infections is warranted.

Some species of the genus *Microascus* are known to be opportunistic pathogens, mainly causing superficial tissue infections, and they represent some of the principal causes of non-dermatophytic onychomycoses. As to *Microascus*, the morphological and molecular identification of the etiological agent has not yet been fully established. *Microascus cirrosus* (*M. cirrosus*) species account for only 2.1% of the genus and are rare isolates of clinical origin, whereas they induce the majority of human infections among the *Microascus* genus (11). To the best of the authors' knowledge, *M. cirrosus*

Curzi was reported to cause the first disseminated infection in a pediatric bone marrow transplant recipient in 1994 (12). Currently, there are a few species of *M. cirrosus* which have been publicly reported to cause human cutaneous and pulmonary infection (10,12-16). The majority of these were determined by cultivation and morphological recognition. The morphological identification of the etiological agent has not been confirmed at the molecular level, and the real prevalence of *M. cirrosus* species in clinical infection remains unknown.

Over the past decades, the development of molecular diagnostic technology has greatly improved the efficiency of pathogen detection in human infections. Notably, metagenomic next-generation sequencing (mNGS) has been widely used to diagnose lung infections in immunocompromised adults (17-21). In the present study, extensive conventional microbiologic testing and mNGS failed to identify *Microascus* species, challenging the accurate diagnosis and individualized therapy of pulmonary fungal infection in the patient. In the present study, a retrospective analysis of the detailed process assisted in the identification and optimal management of fatal lung infection caused by *Microascus* species. Complete laboratory identification methods from morphology to gene sequencing were established to identify the invasive fungal infection by *Microascus* in immunosuppressive patients following haplo-HSCT, including growth and morphological features, extensive drug resistance, the first whole genome information, genetic evolution, protein fingerprint and pathological characteristics. This provides necessary etiological information for investigating the real prevalence of *Microascus* infection in immunosuppressive patients, as *Microascus* is widely distributed worldwide (22,23), and China has the largest HSCT population (24).

Materials and methods

Fungal isolation. Fiberoptic bronchoscopy was performed on the patient at Dushu Lake Hospital Affiliated to Soochow University, Suzhou, China and bronchoalveolar lavage fluid (BALF) was collected from the infected area (left upper bronchus) for laboratory examination, including bacterial culture, 1,3-β-D-glucan (GM) test and mNGS on March 10, 2021. The BALF was inoculated according to the method of bacterial culture, and cultured on a Columbia blood agar plate (Autobio Diagnostics Co., Ltd.) and chocolate agar plate (Autobio Diagnostics Co., Ltd.) at 35˚C and 5% CO_2. Dozens of white filamentous-like fungal colonies were formed on the plate and one pure fungal colony was transferred to Sabouraud agar (Autobio Diagnostics Co., Ltd.) for fungal culture at 28˚C and 35˚C.

Morphological and physiological assessments. Due to the lack of the whole genome of *M. cirrosus* in the National Center for Biotechnology Information (NCBI) database, mNGS testing (BGI) did not include its genetic information. Due to the lack of protein fingerprint information of the fungi, rapid identification methods, such as matrix-assisted laser desorption/ionization (MALDI)-time-of-flight (TOF)-mass spectrometry (MS; IVD MALDI Biotyper System; Bruker Daltonics; Bruker Corporation) could not identify the species. The fungus was inoculated on a chocolate agar plate, Columbia blood plate, nutrient agar, Sabouraud agar and Luria-Bertani (LB) broth [Sangon Biotech (Shanghai) Co., Ltd.] respectively, to observe the growth status of the colony every day. The conidia and septate hyphae were observed in all visual fields under an Olympus CX33 light microscope (Olympus Corporation) with lactophenol cotton blue (BaSO Diagnostics Inc.) staining.

Resistance to common antifungal drugs. Broth dilution antifungal susceptibility testing was performed according to the Clinical and Laboratory Standards Institute (CLSI) M38-A2 (25). In total, four types of antifungal agents were tested, including amphotericin B (CAS: 1397-89-3; Bio Basic, Inc.), caspofungin acetate (CAS: 179463-17-3; Beijing Jin Ming Biotechnology Co., Ltd.), fluconazole (CAS: 86386-73-4; Rhawn Reagent) and fluorocytosine (CAS: 2022-85-7; Rhawn Reagent). Different reagent grades were tested in the following concentrations according the manufacturers' instructions: Amphotericin B 0.03-16 μg/ml, caspofungin 0.03-16 μg/ml, fluconazole 0.12-64 μg/ml, fluorocytosine 0.12-64 μg/ml. The susceptibility of this fungus to each drug was determined.

Multi-site sequence analysis. To accurately identify the fungus, four nuclear DNA regions were amplified and sequenced. Including large subunit ribosomal RNA gene (LSU) and internal transcribed spacer (ITS) regions of the rRNA operon, fragments of the translation elongation factor 1α (EF-1α) and β-tubulin genes (TUB), following the criteria described in the study by Sandoval *et al* (26). DNA extraction was conducted using the Ezup Column Fungi Genomic DNA Purification kit [Sangon Biotech (Shanghai) Co., Ltd.] following the manufacture's protocols. Next, 2X SanTaq PCR Mix [Sangon Biotech (Shanghai) Co., Ltd.], the aforementioned primers , fungal nucleic acid and pure water were added to the PCR reaction tube to yield a total volume of 50 μl, which was amplified on a SLAN-96P (Shanghai Hongshi Medical). The reactions were performed according to the following conditions: 1 cycle at 95˚C for 5 min, followed by 40 cycles at 95˚C for 5 sec, 52-58˚C for 30 sec, 72˚C for 30 sec. The amplification was carried out with the primers, as previously described by Brasch *et al* (27). The PCR product was entrusted to Sangon Biotech (Shanghai) Co., Ltd. for Sanger sequencing and the sequencing instrument used was the Applied Biosystems 3730XL (Applied Biosystems; Thermo Fisher Scientific, Inc.). Consensus sequences obtained for each locus were aligned with sequences of *Microascus* species retrieved from GenBank (http://www.ncbi.nlm.nih.gov/genbank/), using the ClustalW algorithm under MEGA-X v10.0.4 software (28,29). Phylogenetic reconstructions by maximum likelihood (ML) approaches were performed using MEGA-X v10.0.4. The fungal nucleic acid was amplified by PCR with the primers (Table I), as previously described by Brasch *et al* (26,27). and four products were obtained (LSU568bp, ITS618bp, EF-1α898bp and TUB523bp).

Genomic DNA extraction and whole genome sequencing. The fungus was cultured in LB broth for ~3 days, forming a white, pom-pom-shaped fungus. The fungal mass was collected by centrifugation (4˚C and 10,000 x g for 10 min) and washing with saline. The cell wall was destroyed by grinding in liquid nitrogen. The Ezup Column Fungi Genomic DNA Purification kit [Sangon Biotech (Shanghai) Co., Ltd.] was used to extract

Table I. Primer list.

Gene	Primer sequence (5'-3')
NL1-F	GCATATCAATAGCGGAGGAAAAG
NL4-R	GGTCCGTGTTTCAAGACGG
ITS5-F	GGAAGTAAAAGTCGTAACAAGG
ITS4-R	TCCTCCGCTTATTGATATGC
EF1T-F	ATGGGTAAGGARGACAAGAC
1567R-R	ACHGTRCCRATACCACCSATCTT
Bt2a-F	GGTAACCAAATCGGTGCTGCTTTC
Bt2b-R	ACCCTCAGTGTAGTGACCCTTGGC

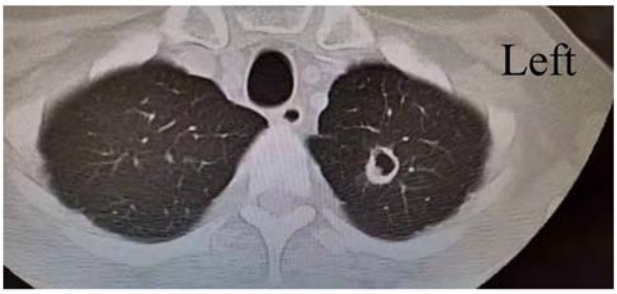

Figure 1. Lung computed tomography of the patient described in the present study.

genomic DNA according to the manufacture's protocols for library construction and next-generation sequencing.

A DNA library with a 500 bp insert size was constructed and sequenced in Illumina's HiSeq platform (Illumina, Inc.) with a pair-end 150 bp sequencing strategy. The sequence reads were assembled using SPAdes v3.5.0 (30). The Protein Coding Genes and rRNA of *M. cirrosus SZ 2021* were then predicted by Prokka (31). The toxicity factors of *M. cirrosus SZ 2021* were analyzed by PHIB-BLAST (http://phi-blast.phi-base.org/). Genome sequencing and analysis were performed by Sangon Biotech (Shanghai) Co., Ltd. As there is currently no whole *M. cirrosus* genome available for reference in the NCBI database, the assembled sequence of *M. cirrosus SZ 2021* was uploaded onto the NCBI public database for research. The mNGS sequence of the patient's sample was aligned with the genome sequence of *M. cirrosus* SZ 2021 using Burrows-Wheeler Aligner software (bwa-0.7.17) (32).

Identification by MALDI-TOF-MS. For sample preparation, briefly, after the fungi were cultured in Yeast Malt Broth, at 35˚C for 2 days; the samples were transferred to Eppendorf (EP) tubes containing 1 ml of high-performance liquid chromatography (HPLC) water, washed and pelleted following centrifugation at 25˚C and 8,000 x g for 10 min. The pellet collected was dissolved in 300 μl HPLC water and washed twice using HPLC water. Subsequently, 900 μl ethanol were added and removed following centrifugation at 25˚C at 10,000 x g for 10 min and air-drying. The sample was then transferred to a grinder for grinding and 100 μl of 70% formic acid was injected into the grinder for ~5 min. The homogenate was then transferred to a clean 1.5-ml EP tube, and an equal amount of acetonitrile was added followed by centrifugation (25˚C and 10,000 x g for 10 min) again. A total of 1 μl of the supernatant was pipetted onto the target, overlaid with 1 μl α-cyano-4-hydroxycinnamic acid matrix and analyzed using MALDI-TOF-MS (Bruker Daltonics; Bruker Corporation). A MBT Compass Explorer (Bruker Daltonics; Bruker Corporation) was used for the analysis of the results.

Murine models of pulmonary infection caused by M. cirrosus. Male C57BL/6 mice (6 weeks old; weight 18±1 g; n=12) were purchased from Xinchen Biotechnology Co. Ltd. The animals were housed in controlled temperature (24±1˚C) and humidity (40-60%) under a natural 12 h/12 h light/dark cycle, with standard chow and water provided *ad libitum*. All animal experiments were carried out in accordance with the National Institute of Health guide for the care and use of laboratory animals (33).

The mice were randomly divided into four groups, with three mice in each group. One group served as a healthy control, while another group was directly infected with *M. cirrosus*. The remaining two groups received 1 mg/kg tacrolimus (FK506) intraperitoneally every day, as previously described (34); of these groups, one was used to establish a pulmonary infection model caused by *M. cirrosus*. For infection, the mice were lightly anesthetized by the inhalation of isoflurane (2% concentration, approximately 2-3 min) and immobilized in an upright position using rubber bands attached to a cardboard for oropharyngeal aspiration. A blunt 24G needle attached to a 1-ml syringe was advanced into the trachea to deliver the indicated number of conidia ($5x10^8$) in a volume of 0.05 ml saline. After 48 h, the mice were then painlessly sacrificed by cervical dislocation. The absence of a heartbeat and pupil dilation for 5 min was used to confirm mortality. The experimental procedures were performed in accordance with the conditions specified and approved by the Animal Experimentation Ethics Committee of Dushu Lake Hospital affiliated to Soochow University (Suzhou, China; approval no. 220138).

Analysis of M. cirrosus SZ 2021-challenged mice. The concentration of IL-6 in serum samples was measured using enzyme linked immunosorbent assay (ELISA) according to the manufacturer's instructions [cat nos. EK206/3-96; Multisciences (Lianke) Biotech Co., Ltd.]. In colony forming unit (CFU) assays, the half of the left lung tissue was harvested and homogenized with glass beads on a Mini-Bead beater (KZ-II; Wuhan Servicebio Technology Co., Ltd.), and serially diluted onto chocolate agar plates in duplicate, and the CFU was determined after 3 days. The remaining lung tissue was immersed in formalin liquid for histological analysis. Paraffin-embedded sections (4 μm) prepared from the lungs of these mice were stained with hematoxylin and eosin (H&E) at room temperature for the evaluation of airway inflammation. Specifically, after dewaxing using xylene, the slices were treated with different alcohol concentrations (100, 100, 95 and 85%, for 1 min each), and then stained with hematoxylin for 10 min after being washed with water. The slices were differentiated with 1% hydrochloric acid alcohol for 5 sec, and then different concentrations of alcohol (95 and 95%, for 10 sec each; 100 and 100%, for 30 sec each) were used for dehydration after washing with water. Following this, the slices were treated with xylene for transparency and sealed with neutral

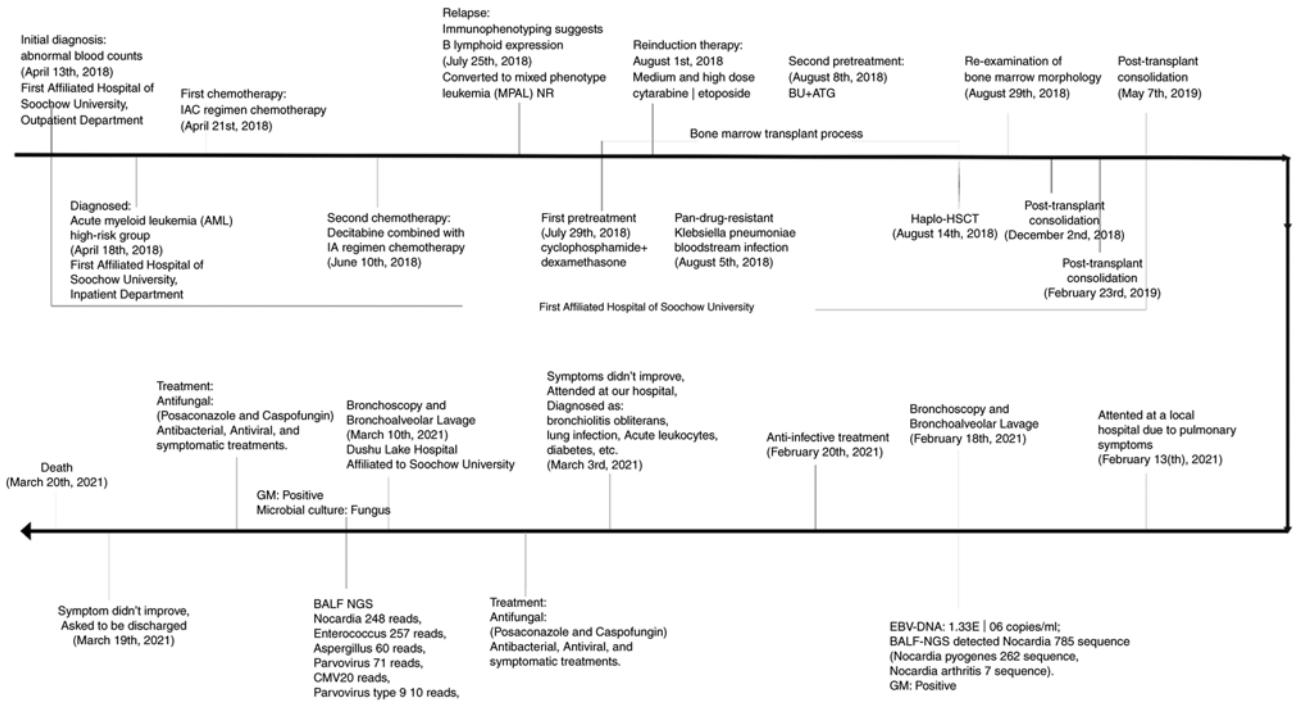

Figure 2. The course record of the case described in the present study.

gum. Olympus BX43 light microscope (Olympus Corporation) was used to capture images from all visual fields.

Statistical analysis. Data are expressed as the mean ± standard error of the mean (SEM). The Student's t-test assuming equal variances was performed to examine the differences between groups and associations were investigated using regression analysis. $P<0.05$ was considered to indicate a statistically significant difference. Data were analyzed using GraphPad prism 8 (Dotmatics).

Results

Isolation of M. cirrosus from the patient. A 40-year-old male was diagnosed with acute myeloid leukemia in a high-risk group on April 18, 2018 and underwent two rounds of chemotherapy. On August 14, 2018, the patient received haplo-HSCT, and the transplant was successfully reconstructed on August 29, 2018. During this time, he continued immunosuppressive therapy with anti-rejection agent (cyclosporine, 50 mg, twice a day) for 3 years in order to prevent GVHD. The patient did not relapse with any hematonosis. Therefore, he was admitted to a local hospital due to aggravated pulmonary symptoms on February 13, 2021, with self-reported 'chest tightness and asthma over the past 6 months, which worsened half a month ago'. He was transferred to Dushu Lake Hospital Affiliated to Soochow University on March 3, 2021 as his pulmonary infection symptoms did not improve following anti-infection treatment at the local hospital. Following admission, the doctor systematically inquired about the medical history and performed relevant examinations. A chest computed tomography (CT) examination presented one infectious cavity in the upper lobe of the left lung (Fig. 1). In addition, the scattered small dots and patches in both lungs were new foci. A number of routine laboratory examinations also suggested infection. To identify the pathogens, a fiberoptic bronchoscopy was performed to collect BALF from left upper bronchus for culture, GM and mNGS on March 10, 2021. Given these findings, posaconazole and caspofungin were used for antifungal therapy, meropenem and co-sulfamethoxazole for antibacterial, ganciclovir and ribavirin for antiviral. Antifungal drugs had been used for ~2 weeks, as clinical symptoms, CT examination and laboratory examinations suggested fungal infection in the lung. Finally, all these therapies failed to control this fatal pulmonary infection, and the patient succumbed due to respiratory failure on March 20, 2021. The patient's disease progression is presented in Fig. 2. In combination with the patient's medical history, symptoms and laboratory tests, the patient was finally diagnosed with the following: i) Bronchiolitis obliterans; ii) lung infection; iii) respiratory failure; iv) acute leukocytes; v) status of hematopoietic stem cell transplantation; vi) chronic GFHD; vii) diabetes; viii) electrolyte disorder; and ix) hypoalbuminemia. The treatment of this patient was based on the study by Williams (35). The 5-year survival rate of patients with bronchiolitis obliterans is not high (36), and the mortality of this patient may be a result of disease progression. *M. cirrosus*, as an infectious factor, is likely to be one of the critical factors that promoted the progression and deterioration of the disease in this patient.

Results of laboratory tests for the patient. Blood cell analysis suggested mild anemia (hemoglobin, 106 g/l; reference range, 130-175 g/l) with a normal white blood cell count ($4.82x10^9$/l; reference range, 3.5-$9.5x10^9$/l; neutrophils, $4.42x10^9$/l; reference range, 1.8-$6.3x10^9$/l; lymphocytes, $0.27x10^9$/l; reference range, 1.1-$3.2x10^9$/l). As to inflammatory markers, the level of procalcitonin was 0.18 ng/ml (reference range, <0.05 ng/ml) and that of hypersensitive C-reactive protein (hs-CRP) was

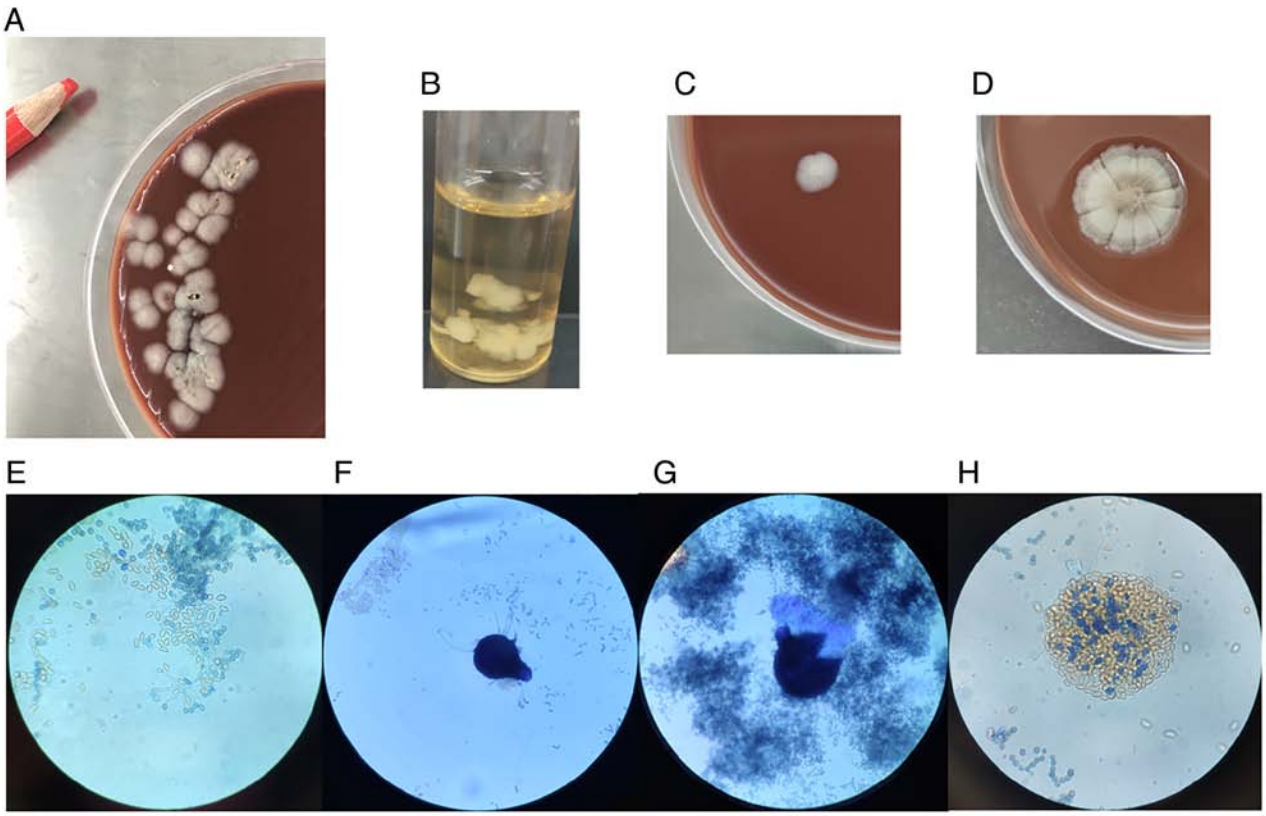

Figure 3. Growth and morphological features of the fungus. (A) Fungal colonies at 3 days of culture for the first time, from the bronchoalveolar lavage fluid of the patient. (B) Growth in LB broth. (C) Colony morphology of *M. cirrosus SZ 2021* cultured on chocolate medium for 3 days. (D) Colony morphology of *M. cirrosus SZ 2021* cultured on chocolate medium for 1 week. (E) The conidia and septate hyphae were observed under a microscope (magnification, x1,000) following staining with lactophenol cotton blue. (F and G) Morphology of ascoma following lactophenol cotton blue staining under a light microscope (magnification, x400). (H) Ascospores: pale yellow parts, crescent-shaped, not blue-stained (magnification, x1,000). *M. cirrosus, Microascus cirrosus*.

59.33 mg/l (reference range, 0-6 mg/l); significantly increased. No significant abnormalities were found in blood coagulation functions. Liver and kidney functions exhibited mild abnormality, 9.03 mmol/l uric acid (reference range, 3.1-8 mmol/l) and 82 U/l alanine transaminase (reference range, 9-50 U/l). Sputum was repeatedly subjected to bacterial culture and no pathogenic microorganisms were found. BALF was collected on February 18, 2021. GM tests were positive (5.65; reference range, <0.5) and mNGS presented *Nocardia nova* with 785 reads, cytomegalovirus with 109 reads, Epstein-Barr virus with 26 reads in this BALF. As symptoms worsened, BALF from the left upper bronchus was collected on March 10, 2021 for mNGS. *Nocardia nova* (248 reads), *Enterococcus* (257 reads), *Aspergillus* (60 reads), parvovirus (71 reads) and cytomegalovirus (20 reads) were detected by mNGS in the BALF. Some white velvety colonies grew in the BALF following 3 days of incubation (Fig. 3), with no evidence of mycobacterial, or additional fungal pathogens. As the accurate morphology of this fungus had not been established and *M. cirrosus* was not listed in the MALDI-TOF-MS library, this fungus was not correctly identified as a *Microascus* species until 1 month later. Numerous results presented some fungal infection in the lungs, including GM, mNGS and pure fungal colonies.

Morphological and physiological characteristics of the fungus. The fungus was detected from the BALF of the patient by growing in both a Columbia blood plate and chocolate agar plate for 2 days. The primary colonies formed on chocolate agar plate were white and 3-4 mm in diameter (Fig. 3A). The fungus was then incubated on a number of media to observe growing at different temperatures. The fungus could grow on a Columbia blood plate, chocolate agar plate, nutrient agar, Sabouraud agar and LB broth (Fig. 3B), and grew well at 35 and 28˚C. It could grow at a more rapid rate and into a larger size on a chocolate agar plate compared with Sabouraud agar. With prolonged cultivation, it presented different conies. Overall, white colonies 3-4 mm in diameter could be observed on the chocolate agar plate for 3 days (Fig. 3C). Colonies >12 mm in diameter with folds around the periphery and a dark pigment in the center could be observed on the culture medium for ~1 week (Fig. 3D). The fungus could also grow at the bottom of a liquid medium. After ~1 week of cultivation on chocolate agar, the ball-shaped, smooth conidia and septate hyphae could be observed under the microscope by staining with lactophenol cotton blue (Fig. 3E). For ~4 weeks, in the dark and brown part of the fungal colony, ascoma and ascospores were observed as the forms of sexual reproduction of the fungus. Microscopically, the ascoma were large and spherical-shaped, containing ascospores which were half-moon shaped (Fig. 3F-H). Based on the presence of branched conidiophores bearing cylindrical anniellids in brush-like groups and on the development of small black ascomata (cleistothecia) after 4 weeks, it was morphologically identified as *Microascus* spp. Compared

Table II. Summary of patients with *Microascus cirrosus*.

First author/s, year	*Microascus* species	Infection Site	Type of transplant or other factors	Age/Sex and area	Antifungal agent or therapeutic methods	Outcome	(Ref.)
de Vroey, 1992	*Microascus cirrosus*	Toenail	No	56/F (Belgium)	Imidazole griseofulvin ketoconazole	Not cured	(13)
de Vroey, 1992	*Microascus cirrosus*	Toenail	No	63/F (Italy)	Griseofulvin miconazole	Not cured	(13)
Krisher, 1995	*Microascus cirrosus*	Lung	AML, Auto-BM	12/M (America)	AMB	No recurrence	(12)
Ustun, 2006	*Microascus cirrosus*	Lung	AML, BMT	49/M (America)	VOR, AMB and TER; Surgery	Succumbed due to AML relapse during infection	(14)
Miossec, 2011	*Microascus cirrosus*	Multiple organs	SOT for cystic fifibrosis	36/M (France)	VOR and CAS	Succumbed (9 days)	(10)
Taton, 2018	*Microascus cirrosus*	Lung	Bilateral lung transplant	60/F (Belgium)	VOR, CAS, TER and AMB	Cure	(15)
Gao, 2018	*Microascus cirrosus*	Left ankle skin	Systemic corticosteroids for two months	17/F (China)	itraconazole	Cure	(16)
Present case	*Microascus cirrosus* SZ 2021	Lung	MPAL, haplo-HSCT	40/M (China)	POS and CAS	Succumbed	Present case

AML, acute myelocytic leukemia; Auto-BMT, autologous bone marrow transplantation; SOT, solid organ transplant; MPAL, mixed phenotype acute leukemia; haplo-HSCT, haploidentical hematopoietic stem cell transplantation; AMB, amphotericin; POS, posaconazole; TER, terbinafine; VOR, voriconazole; CAS, caspofungin; BMT, bone marrow transplant; M, male; F, female.

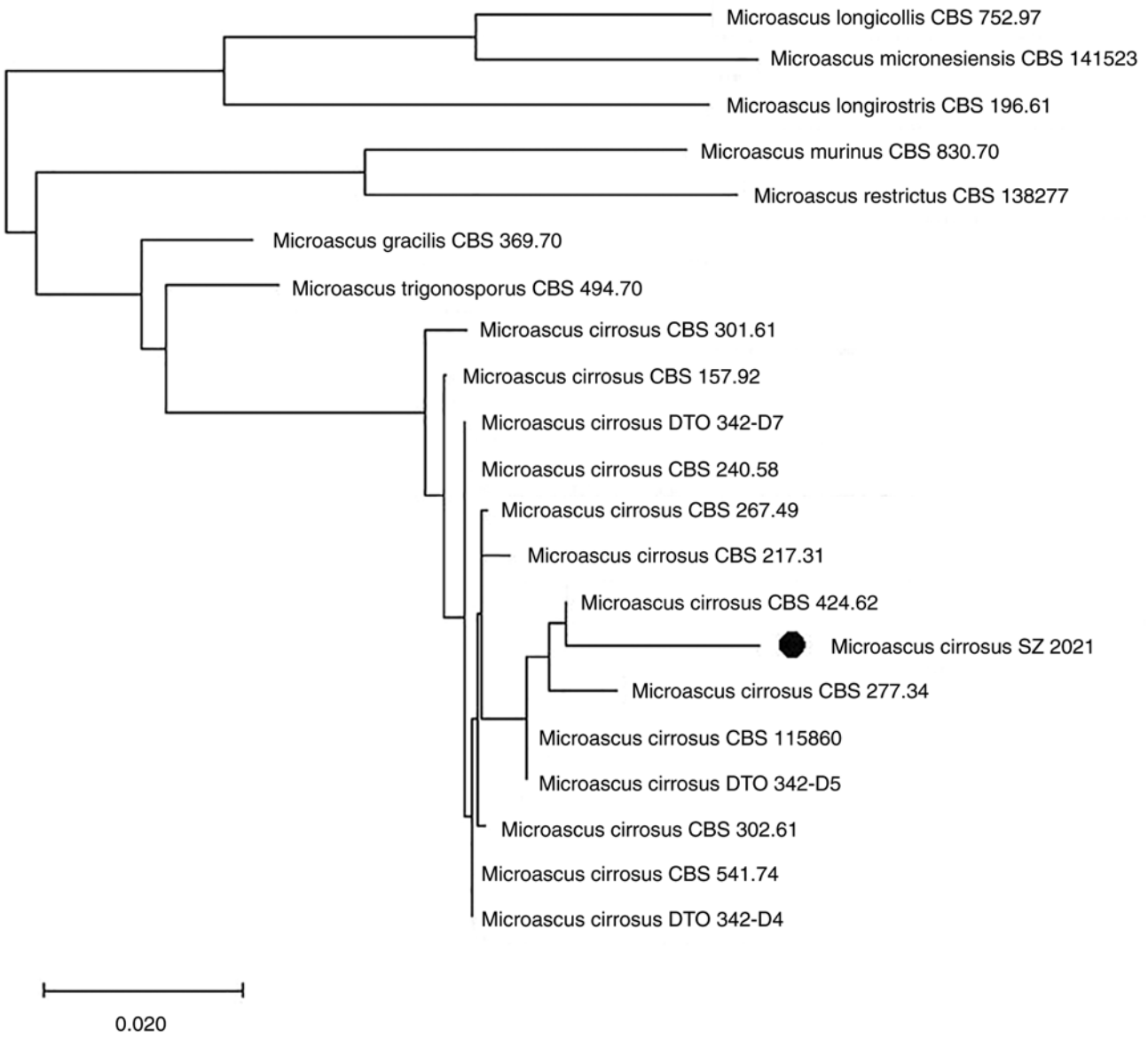

Figure 4. *M. cirrosus SZ 2021* is the fungus described in the present study. The tree diagram constructed by four genes (LSU and ITS regions of the rDNA operon, fragments of the EF-1α and TUB genes) illustrates that the fungus belongs to a new genotype of *M. cirrosus*. *M. cirrosus*, *Microascus cirrosus*; LSU, large subunit ribosomal RNA gene; ITS, internal transcribed spacer; EF-1α, translation elongation factor 1-α; TUB, β-tubulin gene.

with the morphological description of *M. cirrosus* from seven clinical cases (Table II), the *M. cirrosus* presented typical colonies and a microscopic morphology. Compared with other filamentous fungi, such as *Aspergillus*, *Microascus* species usually only have short chains of conidia without apical cysts.

Fungal drug sensitivity. The minimum inhibitory concentrations of this fungus against amphotericin B, caspofungin, fluconazole and fluorocytosine were as follows: Amphotericin B ≥16 μg/ml, caspofungin ≥16 μg/ml, fluconazole ≥64 μg/ml, fluorocytosine ≥64 μg/ml, according to previously published criteria (25). The fungus are insensitive to the antifungal drugs, suggesting that the treatment with common antifungal drugs may be ineffective. This is generally consistent with the results of *in vitro* drug susceptibility studies on *Microascus* spp. by Sandoval-Denis *et al* (11) and Gao *et al* (16).

Multi-site sequence analysis. The analysis revealed that this fungus represented a new genotype in the genus closely related to *M. cirrosus* (Fig. 4). Based on its genetic characteristics and on its distinct morphological features, it was proposed as a novel genotype of *M. cirrosus*, termed *M. cirrosus SZ 2021.*

Whole genome sequence of M. cirrosus SZ 2021 by second-generation sequencing. By performing *de novo* sequencing on the case fungus, its whole nucleic acid information was obtained. The total number of bases after quality control were ~32.61 Mb and the GC Bases Ratio was 53.98%. This second-generation sequencing project was deposited in the NCBI under BioProject: PRJNA835605, BioSample: SAMN28105390 and GenBank: JAMBUN000000000. The version described in the present study is version JAMBUN010000000.

According to gene prediction, *M. cirrosus SZ 2021* has a total of 9,939 coding genes, including the virulence gene,

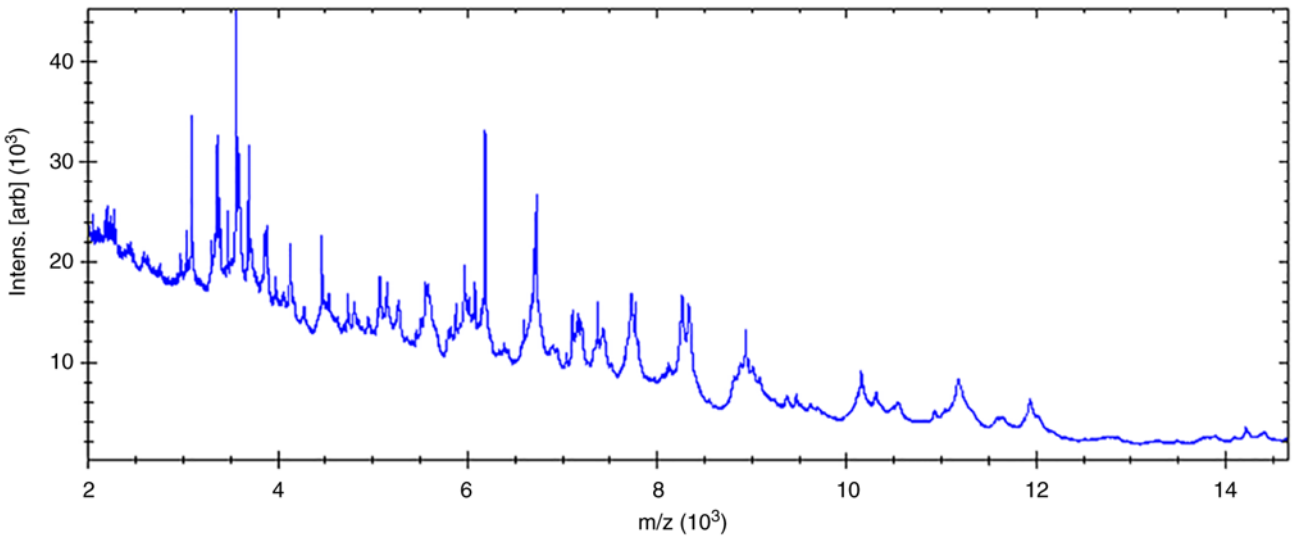

Figure 5. The protein spectra of the *Microascus cirrosus SZ 2021* examined in the present study.

FKS1. Through PHIB-BLAST, it was found that FKS1 of *M. cirrosus SZ 2021* was partially consistent with that of *Aspergillus fumigatus*.

Re-analysis of sequences from BALF detected by mNGS. As no whole genomic information of *Microascus* species were available in public databases, no sequences of this fungus had been reported by mNGS. The results of mNGS from BALF had always recommended *Nocardia* and *Aspergillus* for dozens of reads. The initial mNGS sequence from BALF was reanalyzed by comparing the whole genome sequence of *M. cirrosus SZ 2021*. No *Aspergillus* gene sequence was reported in the former BALF on February 18, 2021 in the local hospital, whereas four reads from *M. cirrosus* could be detected by retrospective bioinformatics analysis. In the BALF sample where the *M. cirrosus* colonies were cultured (March 10, 2021, in Dushu Lake Hospital Affiliated to Soochow University), more than a thousand sequences (1,000 reads) could be aligned, including 660 no-human reads and unclassified reads. The initial BALF mNGS sequence from the patients who underwent HSCT and developed pulmonary infection, but failed to be cured in Dushu Lake Hospital Affiliated to Soochow University were also reanalyzed. Different numbers of sequences of *M. cirrosus* could be detected in another two cases (a 23-year-old male was diagnosed with acute myeloid leukemia and another 31-year-old male was diagnosed with acute lymphoblastic leukemia; both had received HSCT), namely three reads and 13 reads, respectively, with no verification of cultural colonies, but favored by re-analysis of the mNGS sequences. In conclusion, the sequences from BALF detected by mNGS demonstrated that *M. cirrosus* could be detected correctly and rapidly by mNGS, as there is correct genomic information in the database.

Distinguished features of M. cirrosus detected using MALDI-TOF-MS. The protein fingerprint of *M. cirrosus SZ 2021* was obtained by MALDI-TOF-MS (Fig. 5); however, the strain name was not identified, probably as the MS identification database did not contain strain information. Subsequently, a main spectrum profile dendrogram was constructed by combining *M. cirrosus SZ 2021* with other *Microascus* spp., *Aspergillus fumigatus* and *Nocardia nova*. It was found that *M. cirrosus SZ 2021* was relatively close to *Microascus gracilis*, classified as a different cluster from *Aspergillus fumigatus* and *Nocardia nova* (Fig. 6).

Results of animal models of pulmonary infection by M. cirrosus SZ 2021. Prior to sacrifice, one mouse died following infection by *M. cirrosus SZ 2021* in the immunosuppressed group pre-treated with FK506. The H&E-stained sections of the lung tissue also revealed a greater amount of inflammatory cell infiltration in *M. cirrosus*-infected mice from the immunosuppressed group (Fig. 7A). The levels of IL-6, as a prognostic biomarker, which can detect an immediate response to infection compared with hs-CRP and procalcitonin (37), were also examined. Following infection with *M. cirrosus SZ 2021*, it was observed that the IL-6 level was significantly increase in mouse serum ($P<0.05$), particularly in mice pre-treated with FK506 (Fig. 7B). The CFU assays revealed no *M. cirrosus* growth, with the exception of two mice from the immunosuppressed group. The mouse with the highest *M. cirrosus* colony count was the one that died prior to sacrifice (Fig. 7C).

Discussion

In the present study, the discovery of the real pathogenic fungus of *M. cirrosus* posed a challenge, due to the limited knowledge available on the *Microascus* genus. No *Microascus* species were contained in the clinical database, although mNGS is used extensively in China. Only one of the repeated culture tests of sputum and BALF presented some pure fungal colonies and, furthermore, they were not correctly identified as *M. cirrosus* due to limited information. Thus, their extensive drug resistance was not detected and recognized in time and effective therapy was not administered; the patient succumbed due to fatal lung infection, even though antifungal drugs had been used continuously according to the repeated hints of fungal etiology by GM

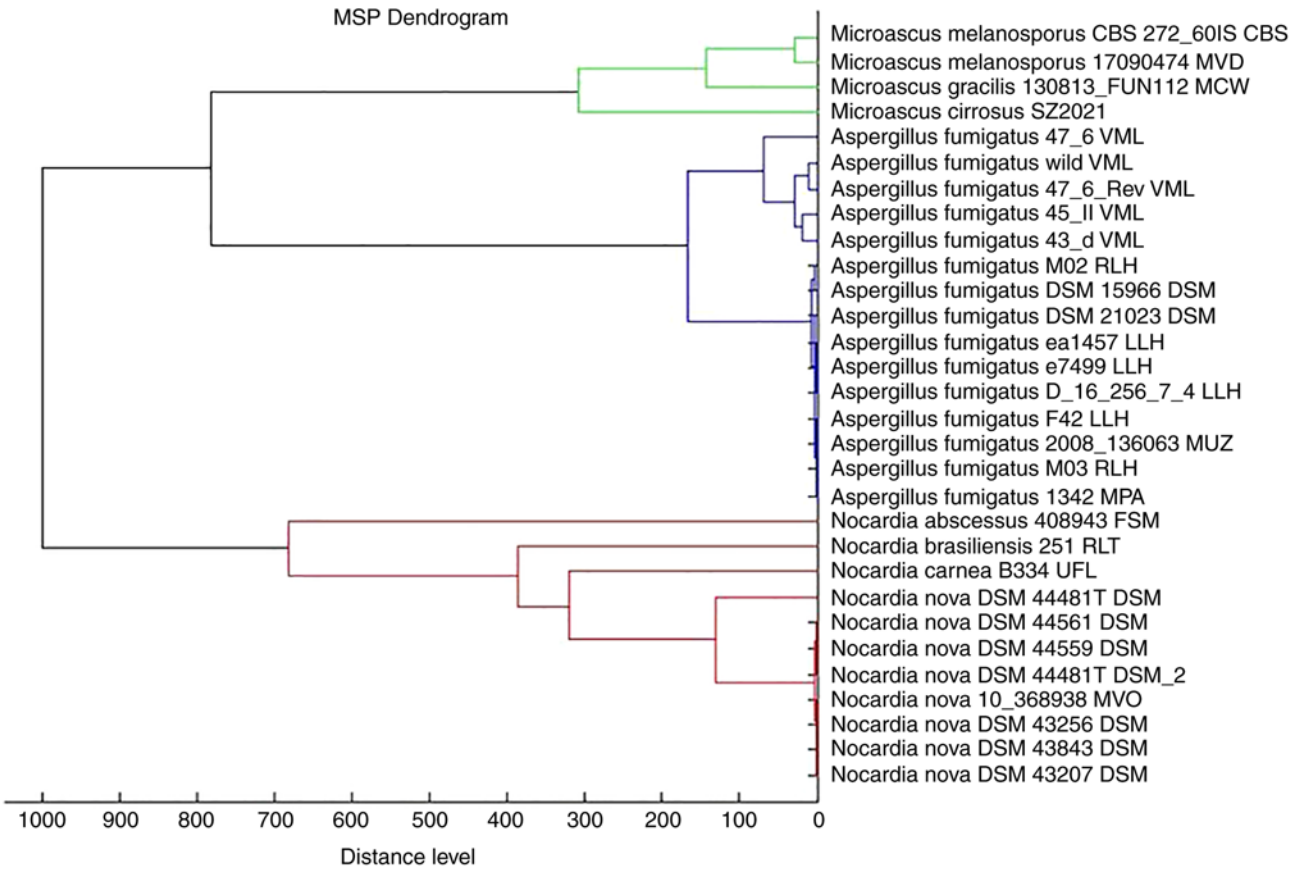

Figure 6. Main spectrum profile dendrogram constructed from protein fingerprints of *Microascus cirrosus SZ 2021*, *Nocardia nova* and *Aspergillus fumigatus*.

tests. Indeed, through retrospective reanalysis of the original sequencing of the first BALF sample by mNGS, DNA sequence fragments of *M. cirrosus* were discovered with 13 reads, which indicated that the patient likely carried this fungus from the beginning. Following treatment with anti-fungal drugs for half a month, *M. cirrosus* spread and replicated proficiently within the lungs due to its extensive drug resistance, conditions which favored its growth. It therefore appears that at times of poor efficacy by routine anti-fungal infection treatment, uncommon fungal pathogens may be misdiagnosed by a single test. Apart from studying the characteristics of *M. cirrosus* in detail, the timely incorporation of *M. cirrosus* into the rapid mass spectrometry identification and gene information database of fungi may be beneficial to improve the correct detection of *M. cirrosus*. As this fungus is mostly resistant to common antifungal drugs, it is difficult to treat. To date, the majority of patients who underwent transplantation and were infected with this fungus were not successfully cured. Perhaps it would be beneficial to examine the use of some uncommon therapies, including the combined use of several antifungal drugs, the surgical resection of localized lesions, and immune regulation therapy (Table II).

Infection with *M. cirrosus* has been reported in the United States, Belgium, France, Italy and China. From the geographical distribution point of view, *M. cirrosus* has been reported as a plant-infecting pathogen with no regional limitation (38). The characteristics of infection are mainly lung and local skin infections, among which lung infections are basically observed in immunocompromised patients, and local skin infections can appear in non-immunocompromised patients. Of note, the majority of fatal lung infections by *M. cirrosus* are difficult to combat successful in the transplant population (Table II). The present study described a case of *M. cirrosus* pulmonary infection, which is known to be the first reported patient undergoing haplo-HSCT in China. To date, to the best of the authors' knowledge, only one case of skin infection of *M. cirrosus* has been reported in China (16). *M. cirrosus* infection mostly occurs in post-transplant population (10,12,14,15), and China has a large transplant population. Based on the whole genome sequence of *M. cirrosus*, the present study retrospectively reanalyzed the initial BALF mNGS sequence from patients who underwent HSCT and suffered from fatal pulmonary infection, but failed to be cured at Dushu Lake Hospital Affiliated to Soochow University. Different numbers of sequences of *M. cirrosus* could be detected in another two cases, three and 13 reads respectively, favoring the fungal etiological diagnosis by GM tests. The data from animal experiments demonstrated that *M. cirrosus* in immunosuppressed mice can cause severe pneumonia, even leading to mortality. Therefore, the correct and rapid diagnosis of the *Microascus* genus in transplant populations is required to fully understand the epidemiology of this fungal infection.

In the present study, the GM test and mNGS suggested that the patient had a pulmonary fungal infection; however, this clinical isolate was misdiagnosed. Finally, the fungus was identified by culture, although this was time-consuming and treatment was delayed. The development of mNGS and its wide application in the diagnosis of infectious diseases have broken the existing limitations of conventional diagnostic

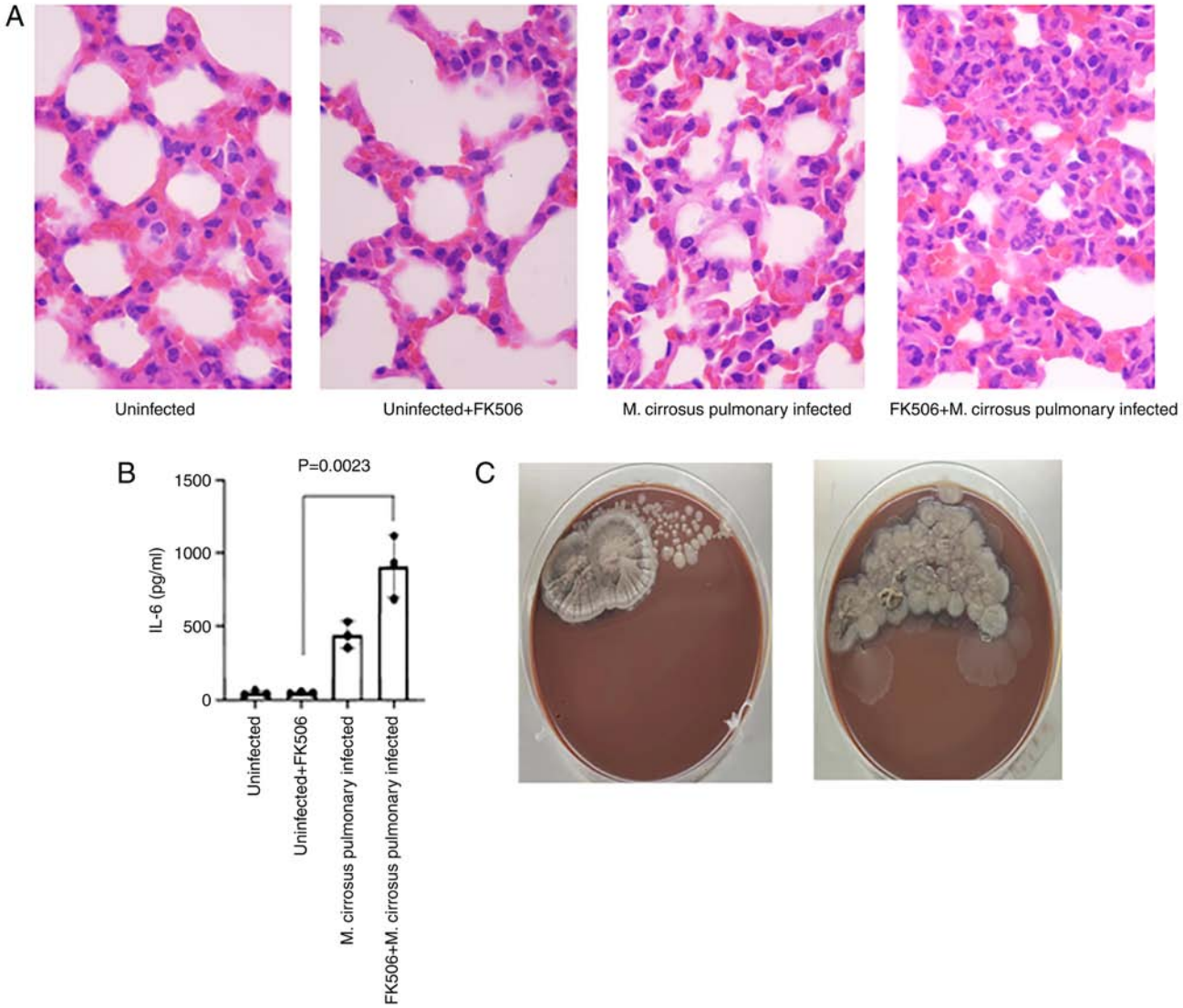

Figure 7. Results of pulmonary infection by *M. cirrosus SZ 2021 in mice*. (A) Histological sections (stained with H&E) representative photomicrographs of H&E-stained sections from formalin-fixed and paraffin-embedded lung tissues of mice (magnification, x1,000). (B) The serum concentration of IL-6 in murine models. (C) Determination of colony forming units in the experimental group. H&E, hematoxylin and eosin.

approaches (39). Since mNGS does not require live pathogens or cultures, its positive rate can be much higher than conventional diagnostic approaches, and the types of pathogens that can be detected are wider than those of conventional methods (40). Thus, mNGS is more suitable for the diagnosis of opportunistic pathogens and mixed infections in immunosuppressed patients. However, metagenomic sequencing technology also has disadvantages, such as higher costs, more complex procedures, the background of human-derived nucleic acids, and the need for continuous updating of databases (41,42). The present study reported a case of *M. cirrosus*, which was not regarded as a pathogen in bioinformatics analysis using mNGS. The reasons for this may be as follows: i) *M. cirrosus* is considered to be a Biological Safety Level one grade environmental microorganism, such as *M. cirrosus CBS217.31* (https://wi.knaw.nl/details/80/9762), thus, its partial sequence information is not included in the database for mNGS analysis; ii) there is currently no genome information of *M. cirrosus* in the NCBI database. This may lead to the wrong detection or undetected infection in immunosuppressed groups.

For this case, the assembled sequence of *M. cirrosus* was provided and it was uploaded onto the NCBI public database for research. In addition, a number of sequences of this fungus could be detected by retrospective analysis of the mNGS results of BALF. Thus, these data facilitate the rapid detection of *M. cirrosus* by mNGS for the effective diagnosis of *M. cirrosus* infection.

Compared with other filamentous fungi, such as *Aspergillus*, *M. cirrosus* was identified with only short chains of conidia without apical cysts in the present study. Due to the limited information available on this fungus, *M. cirrosus* may not be correctly recognized by morphological identification even if it has been cultivated. MALDI-TOF-MS is a common method for the rapid identification of microbial strains. Cultured *M. cirrosus* can be accurately identified MALDI-TOF-MS by a close the protein fingerprint of *M. gracilis,* presenting a very different cluster from *Aspergillus fumigatus* and *Nocardia nova*. Thus, *M. cirrosus* can be rapidly detected by MALDI-TOF-MS.

In conclusion, there is an urgent need for the extensive investigation of the frequency and pathogenicity of *M. cirrosus* in immunosuppressed patients, as systemic *Microascus* infections are difficult to treat and, hence, are frequently fatal. For diagnosis, the establishment of standard morphological and growth criteria is required. The rapid diagnosis of *M. cirrosus* can be reliably achieved by mNGS, if the vital genetic information has been uploaded onto public databases. Due to its frequent and extensive resistance to drugs, attention should be paid to refractory pneumonia due to *M. cirrosus* when routine antifungal therapy is ineffective. In addition, it is also necessary to explore effective treatment methods, as for instance, the surgical removal of infection lesions combined with the use of multiple drugs.

Acknowledgements

Not applicable.

Funding

The present study was financially supported by the Suzhou Science and Technology Planning Project (grant nos. SLT201921, SZM2021011, SZM2021018 and SKY2022091) and the Jiangsu Provincial Key Research and Development Program (grant no. BE2019656).

Availability of data and materials

The datasets used and/or analyzed during the current study are available from the corresponding author on reasonable request. The second-generation sequencing project of *Microascus cirrosus SZ 2021* was deposited in NCBI under BioProject: PRJNA835605 (https://www.ncbi.nlm.nih.gov/bioproject/835605), BioSample: SAMN28105390 (https://dataview.ncbi.nlm.nih.gov/object/SAMN28105390) and GenBank: JAMBUN000000000. The version described herein is version JAMBUN010000000.

Authors' contributions

QH and JC conceived and designed the study. JC and TZ completed the isolation, culture and morphological observation of the strain. DZ provided the cases and data. JC, LZ, XH, TZ, JH, DZ and PZ completed the molecular identification and the data analysis. JC, QH and LW participated in the analysis or interpretation of the data. JC participated in the drafting of the manuscript. LW, JH and QH contributed to the revision of article. QH and LW confirm the authenticity of all the raw data. All authors have read and approved the final version of the manuscript.

Ethics approval and consent to participate

The present study was conducted in accordance with the ethical standards of the Declaration of Helsinki, and was approved by the Institutional Review Board of Dushu Lake Hospital Affiliated to Soochow University (Suzhou, China; approval no. 220138). Informed consent was waived due to the retrospective nature of the study.

Patient consent for publication

Not applicable.

Competing interests

The authors declare that they have no competing interests.

References

1. Penack O, Marchetti M, Ruutu T, Aljurf M, Bacigalupo A, Bonifazi F, Ciceri F, Cornelissen J, Malladi R, Duarte RF, *et al*: Prophylaxis and management of graft versus host disease after stem-cell transplantation for haematological malignancies: Updated consensus recommendations of the European society for blood and marrow transplantation. Lancet Haematol 7: e157-e167, 2020.
2. Kang HG, Zhang D, Degauque N, Mariat C, Alexopoulos S and Zheng XX: Effects of cyclosporine on transplant tolerance: the role of IL-2. Am J Transplant 7: 1907-1916, 2007.
3. Liddicoat AM and Lavelle EC: Modulation of innate immunity by cyclosporine A. Biochem Pharmacol 163: 472-480, 2019.
4. Esquirol A, Pascual MJ, Kwon M, Pérez A, Parody R, Ferra C, Garcia Cadenas I, Herruzo B, Dorado N, Hernani R, *et al*: Severe infections and infection-related mortality in a large series of haploidentical hematopoietic stem cell transplantation with post-transplant cyclophosphamide. Bone Marrow Transplant 56: 2432-2444, 2021.
5. Roberts MB and Fishman JA: Immunosuppressive agents and infectious risk in transplantation: managing the 'net state of immunosuppression'. Clin Infect Dis 73: e1302-e1317, 2021.
6. Ji C, Yang Z, Zhong X and Xia J: The role and mechanism of CARD9 gene polymorphism in diseases. Biomed J 44: 560-566, 2021.
7. Caira M, Trecarichi EM, Mancinelli M, Leone G and Pagano L: Uncommon mold infections in hematological patients: epidemiology, diagnosis and treatment. Expert Rev Anti Infect Ther 9: 881-892, 2011.
8. Mohammedi I, Piens MA, Audigier-Valette C, Gantier JC, Argaud L, Martin O and Robert D: Fatal microascus trigonosporus (anamorph Scopulariopsis) pneumonia in a bone marrow transplant recipient. Eur J Clin Microbiol Infect Dis 23: 215-217, 2004.
9. Baddley JW, Moser SA, Sutton DA and Pappas PG: Microascus cinereus (Anamorph scopulariopsis) brain abscess in a bone marrow transplant recipient. J Clin Microbiol 38: 395-397, 2000.
10. Miossec C, Morio F, Lepoivre T, Le Pape P, Garcia-Hermoso D, Gay-Andrieu F, Haloun A, Treilhaud M, Leclair F and Miegeville M: Fatal invasive infection with fungemia due to Microascus cirrosus after heart and lung transplantation in a patient with cystic fibrosis. J Clin Microbiol 49: 2743-7, 2011.
11. Sandoval-Denis M, Sutton DA, Fothergill AW, Cano-Lira J, Gené J, Decock CA, de Hoog GS and Guarro J: Scopulariopsis, a poorly known opportunistic fungus: Spectrum of species in clinical samples and in vitro responses to antifungal drugs. J Clin Microbiol 51: 3937-43, 2013.
12. Krisher KK, Holdridge NB, Mustafa MM, Rinaldi MG and McGough DA: Disseminated Microascus cirrosus infection in pediatric bone marrow transplant recipient. J Clin Microbiol 33: 735-737, 1995.
13. de Vroey C, Lasagni A, Tosi E, Schroeder F and Song M: Onychomycoses due to Microascus cirrosus (syn. M. desmosporus). Mycoses 35: 193-196, 1992.
14. Ustun C, Huls G, Stewart M and Marr KA: Resistant Microascus cirrosus pneumonia can be treated with a combination of surgery, multiple anti-fungal agents and a growth factor. Mycopathologia 162: 299-302, 2006.
15. Taton O, Bernier B, Etienne I, Bondue B, Lecomte S, Knoop C, Jacob F and Montesinos I: Necrotizing Microascus tracheobronchitis in a bilateral lung transplant recipient. Transpl Infect Dis 20: 2018.
16. Gao L, Chen J, Gao D and Li M: Primary cutaneous infection due to Microascus cirrosus: A case report: BMC Infect Dis 18: 604, 2018.
17. Chiu CY and Miller SA: Clinical metagenomics. Nat Rev Genet 20: 341-355, 2019.

18. Wilson MR, Sample HA, Zorn KC, Arevalo S, Yu G, Neuhaus J, Federman S, Stryke D, Briggs B, Langelier C, *et al*: Clinical metagenomic sequencing for diagnosis of meningitis and encephalitis. N Engl J Med 380: 2327-2340, 2019.
19. Gu W, Deng X, Lee M, Sucu YD, Arevalo S, Stryke D, Federman S, Gopez A, Reyes K, Zorn K, *et al*: Rapid pathogen detection by metagenomic next-generation sequencing of infected body fluids. Nat Med 27: 115-124, 2021.
20. Tang W, Zhang Y, Luo C, Zhou L, Zhang Z, Tang X, Zhao X and An Y: Clinical application of metagenomic next-generation sequencing for suspected infections in patients with primary immunodeficiency disease. Front Immunol 12: 696403, 2021.
21. Azar MM, Schlaberg R, Malinis MF, Bermejo S, Schwarz T, Xie H and Dela Cruz CS: Added diagnostic utility of clinical metagenomics for the diagnosis of pneumonia in immunocompromised adults. Chest 159: 1356-1371, 2021.
22. Issakainen J, Salonen JH, Anttila VJ, Koukila-Kähkölä P, Castrén M, Liimatainen O, Vuento R, Ojanen T, Koivula I, Koskela M and Meurman O: Deep, respiratory tract and ear infections caused by Pseudallescheria (Scedosporium) and Microascus (Scopulariopsis) in Finland. A 10-year retrospective multi-center study. Med Mycol 48: 458-65, 2010.
23. Huang L, Chen W, Guo L, Zhao L, Cao B, Liu Y, Lu B, Li B, Chen J and Wang C: Scopulariopsis/Microascus isolation in lung transplant recipients: A report of three cases and a review of the literature. Mycoses 62: 883-892, 2019.
24. Chang YJ, Pei XY and Huang XJ: Haematopoietic stem-cell transplantation in China in the era of targeted therapies: current advances, challenges, and future directions. Lancet Haematol 9: e919-e929, 2022.
25. Clinical and Laboratory Standards Institute. 2008. Reference method for broth dilution antifungal susceptibility testing of filamentous fungi: approved standard, 2nd ed. CLSI document M38-A2. Clinical and Laboratory Standards Institute, Wayne, PA.
26. Sandoval-Denis M, Gené J, Sutton DA, Cano-Lira JF, deHoog GS, Decock CA, Wiederhold NP and Guarro J: Redefining Microascus, Scopulariopsis and allied genera. Persoonia 36: 1-36, 2016.
27. Brasch J, Beck-Jendroschek V, Iturrieta-González I, Voss K and Gené J: A human subcutaneous infection by Microascus ennothomasiorum sp. nov. Mycoses 62: 157-164, 2019.
28. Thompson JD, Higgins DG and Gibson TJ: CLUSTAL W: Improving the sensitivity of progressive multiple sequence alignment through sequence weighting, position-specific gap penalties and weight matrix choice. Nucleic Acids Res 22: 4673-4680, 1994.
29. Kumar S, Stecher G, Li M, Knyaz C and Tamura K: MEGA X: Molecular evolutionary genetics analysis across computing platforms. Mol Biol Evol 35: 1547-1549, 2018.
30. Bankevich A, Nurk S, Antipov D, Gurevich AA, Dvorkin M, Kulikov AS, Lesin VM, Nikolenko SI, Pham S, Prjibelski AD, *et al*: SPAdes: A new genome assembly algorithm and its applications to single-cell sequencing. J Comput Biol 19: 455-77, 2012.
31. Seemann T: Prokka: Rapid prokaryotic genome annotation. Bioinformatics 30: 2068-2069, 2014.
32. Li H and Durbin R: Fast and accurate short read alignment with Burrows-Wheeler transform. Bioinformatics 25: 1754-1760, 2009.
33. National Institutes of Health (1996) Guide for the care and use of laboratory animals. 7th Edition, National Academy Press, Washington DC.
34. Herbst S, Shah A, Carby M, Chusney G, Kikkeri N, Dorling A, Bignell E, Shaunak S and Armstrong-James D: A new and clinically relevant murine model of solid-organ transplant aspergillosis. Dis Model Mech 6: 643-651, 2013.
35. Williams KM: How I treat bronchiolitis obliterans syndrome after hematopoietic stem cell transplantation. Blood 129: 448-455, 2017.
36. Ditschkowski M, Elmaagacli AH, Koldehoff M, Gromke T, Trenschel R and Beelen DW: Bronchiolitis obliterans after allogeneic hematopoietic SCT: Further insight-new perspectives? Bone Marrow Transplant 48: 1224-1229, 2013.
37. Karakioulaki M and Stolz D: Biomarkers in pneumonia-beyond procalcitonin. Int J Mol Sci 20: 2004, 2019.
38. Mirzaee MR, Asgari B, Zare R and Mohammadi M: Association of Microascus cirrosus (microascaceae, ascomycetes) with brown leaf spot of pistachio in Iran. Plant Dis 94: 642, 2010.
39. Jin X, Li J, Shao M, Lv X, Ji N, Zhu Y, Huang M, Yu F, Zhang C, Xie L, *et al*: Improving suspected pulmonary infection diagnosis by bronchoalveolar lavage fluid metagenomic next-generation sequencing: A multicenter retrospective study. Microbiol Spectr 10: e0247321, 2022.
40. Miao Q, Ma Y, Wang Q, Pan J, Zhang Y, Jin W, Yao Y, Su Y, Huang Y, Wang M, *et al*: Microbiological diagnostic performance of metagenomic next-generation sequencing when applied to clinical practice. Clin Infect Dis 67 (Suppl 2): S231-S240, 2018.
41. Gu W, Miller S and Chiu CY: Clinical metagenomic next-generation sequencing for pathogen detection. Annu Rev Pathol 14: 319-338, 2019.
42. Filkins LM, Bryson AL, Miller SA and Mitchell SL: Navigating clinical utilization of direct-from-specimen metagenomic pathogen detection: Clinical applications, limitations, and testing recommendations. Clin Chem 66: 1381-1395, 2020.